ISBN: 978-3-95450-250-9 ISSN: 2673-5520 doi:10.18429/JACoW-MEDSI2023-THPPP015

MECHANICAL DESIGN OF THE NOVEL PRECISE SECONDARY SOURCE SLITS

X. Yan, J. Liu, Z. Ji, Y. Gong, H. Qin†, Institution of Advanced Science Facilities, Shenzhen, China

Abstract

High-precision slits are extensively adopted in coherent or nano-focusing beamlines as the secondary source, which can accurately define or achieve a beam size at the micron or sub-micron scale, while maintaining high stability. This paper presents the design of a set of precise slits based on a flexure hinge mechanism, which enables a nano-scale resolution and a stroke of hundreds of microns simultaneously. The coarse or fine adjustment motion of each blade can be accomplished with or without a displacement amplification mechanism, which is driven by a piezo actuator. Furthermore, the kinematic and dynamics models are investigated through finite element analysis (FEA) and numerical analysis successively, yielding consistent results. The optimized slits system can provide a linear stroke of up to 400 μm with a resolution of 10 nm both in horizontal and vertical directions, whose first Eigen frequency is 130 Hz.

INTRODUCTION

As an important component of the beamline, the secondary source slit has the function of shaping the beam size and preventing scattering X-rays. With the increasing demands for smaller beam size in hard X-ray beamlines at diffraction-limited storage ring, the performance requirements for secondary source slits have become more challenging [1-2]. The aim of this work is thus the development of an innovative design of a large stroke compact slits system with nano scale beam shaping capability. The following sections will introduce design and analysis of the secondary source slits.

DESIGN OF THE SLITS

Specifications

Table 1: The Overall Specifications of Secondary Source Slits

Item	Specification
Vacuum	$\leq 10^{-9}$ mbar
Y/Z motion range	10 mm
Y/Z resolution	1 μm
Y/Z repeatability	± 2 μm
Parallelism between blades	≤ 0.2 μm
Range of rotary adjustment	± 0.5°
Slits blade motion range	−20 ~ 200 μm (H) −20 ~ 200 μm (V)
Slits resolution	0.01 μm
Slits repeatability	± 0.03 μm

† qinhongliang@mail.iasf.ac.cn

Mechanical Design

The overall slit system consists of five parts, including (1) the slit motion adjustment mechanism, (2) the chamber, (3) the vertical movement (Z direction), (4) the horizontal movement (Y direction) and (5) a marble support, as shown in Fig. 1 (see the specifications in Table 1).

The main mechanism containing slit motion and parallelism adjustment are integrated in a compatibility of ultra-high vacuum (UHV) chamber. There are two sets of slit motion adjustment components, positioned perpendicular to each other and slightly offset along the beam direction. These components enable horizontal and vertical slit openings, with each set comprising two translational mechanisms and one rotating mechanism. Figure 2 shows a motion adjustment assembly. One tungsten carbide blade is mounted on each translational mechanism, which is driven by a piezo actuator via a linear flexure hinge. Two translational mechanisms are symmetrically connected with the inner part of the flexible rotating mechanism, i.e. a circular flexible hinge, by which the pair of blades can be aligned to X-Ray beam accurately. The outer part of the rotating mechanism is fixed on the chamber bottom using silvered screws. Herein, there is a manual flexible hinge mechanism connected to one of the blades for parallelism alignment during installation.

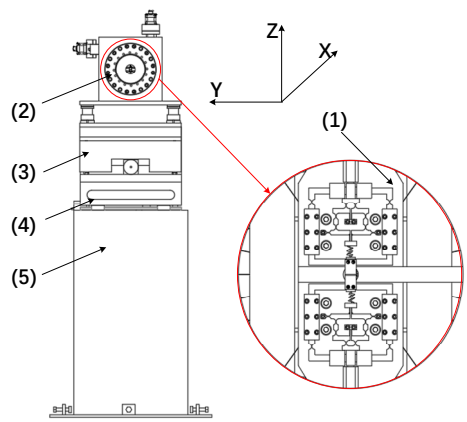

Figure 1: Schematic diagram of the secondary source slits.

There are two operation modes for the slit translational motion, corresponding to coarse or fine adjustment. (1) Displacement amplification mode. When the electromagnets are power-off, then the piezo actuator directly drives the hinge to accomplish the output displacement amplification. The blade fixed on the displacement output structure is connected to the hinge output end with a preload spring. (2) Non-displacement amplification mode. When the electromagnets are charged, it will clamp the rod fixed on the translational hinge input end, the blade is moved directly with the displacement output structure driven by the

ISBN: 978-3-95450-250-9 ISSN: 2673-5520 doi:10.18429/JACoW-MEDSI2023-THPPP015

piezo actuator, guiding by a pair of rails. The slit blade has a good output displacement response when the piezo actuator step scans with a step size of 10 nm.

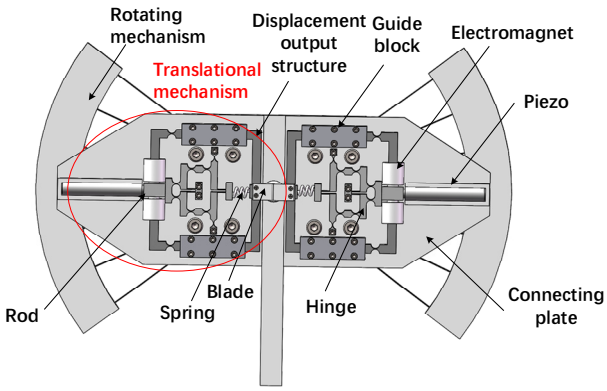

Figure 2: Motion adjustment mechanism.

The whole chamber is installed on two motorized stages, which have a motion stroke of 10 mm both in horizontal and vertical direction for alignment. A stable marble support is underneath the stages, isolating vibrations from the floor.

Analysis and Results

As illuminated in Fig. 3, the flexible hinge structure is the core of the slit displacement amplification mechanism. The working principle is described as follows.

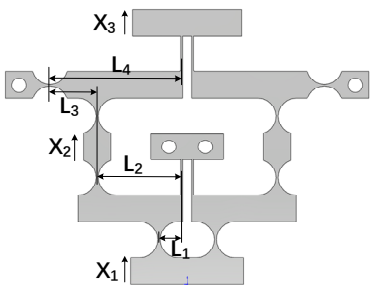

Figure 3: Two-stage lever-type flexure hinge mechanism.

The input displacement X_1 is driven by the piezo actuator, and the first-stage output displacement is X_2 with an amplification factor of L_2/L_1. Similarly, taking X_2 as the input displacement of the second lever-type hinge mechanism, the output displacement X_3 is obtained since the second amplification factor is L_4/L_3. Therefore, the total amplification ratio of the hinge mechanism is:

$$\frac{X_3}{X_1} = \frac{L_2}{L_1} \times \frac{L_4}{L_3} . \quad (1)$$

To meet the requirement for the secondary source slits, a comprehensive consideration of a linear stroke up to 200 µm, single nanometre resolution, and high stiffness are taken into account. The final amplification factor is 10 after optimizing the lever lengths. The static analysis of the translational mechanism is carried out by finite element method, and the maximum output displacements in two modes are 200 µm and 20 µm respectively while the input displacements varying from 1 to 20 µm, as shown in Fig. 4. Furthermore, analytical solutions are calculated. The relationship between input and output displacement of the translational mechanism in the two modes are depicted in Fig. 5. It can be seen that the finite element simulation results are in good consistent with the analytical ones, and the output-input displacement ratio is close to 10 in displacement amplification case. It is noteworthy that there is a slight deviation when the input displacement is greater than 14 µm, which may be due to the accumulated stress resulting from larger deformation. It is negligible because even the maximum deviation accounts for only 1 percent. In non-displacement amplification case, it works perfectly with a high resolution.

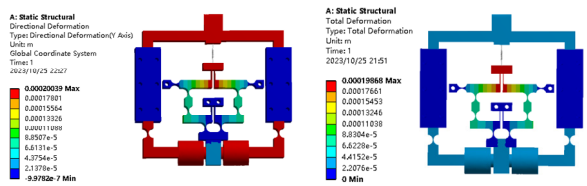

(a) (b)

Figure 4: Translational mechanism displacement with input displacement of 20 µm. (a) Displacement amplification mode (b) Non-displacement amplification mode.

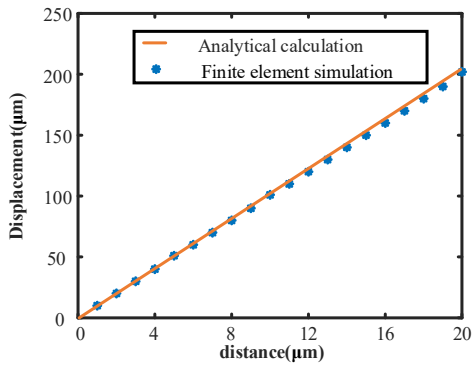

(a)

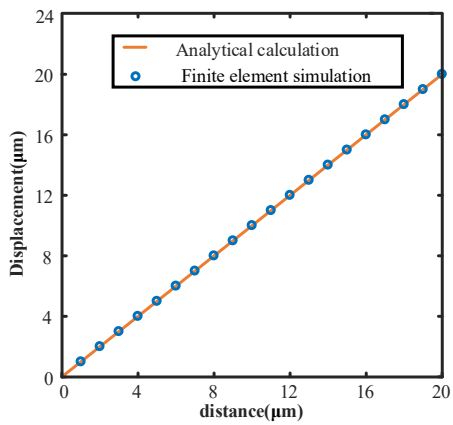

(b)

Figure 5: Input-output displacement curve of translational mechanism in two modes. (a) Displacement amplification mode. (b) Non-displacement amplification mode.

ISBN: 978-3-95450-250-9 ISSN: 2673-5520 doi:10.18429/JACoW-MEDSI2023-THPPP015

Considering the stress in the hinge as another determining factor, it is necessary to compromise the maximum stress below about 50 % of the yield strength of the material when the hinge deflects to the needed motion limit. QBe2 and 17-7PH stainless steel are chosen as the material of translational and rotating hinges respectively, and the equivalent stress results are shown in Fig. 6. Figure 6 (a) indicates that the maximum von Mises stress of translational hinges in non-displacement amplification case is 452.6 MPa while applying an input displacement of 20 µm. Figure 6 (b) indicates that the maximum von Mises stress of translational hinges in displacement amplification case is 452.1 MPa while applying an input displacement of 20 µm. Figure 6 (c) shows that the maximum von Mises stress of the rotating hinges is about a half of its yielding stress set as 171 MPa while applying a torque of 0.5 Nm. The maximum actuated rotary movement is about 0.55 degree.

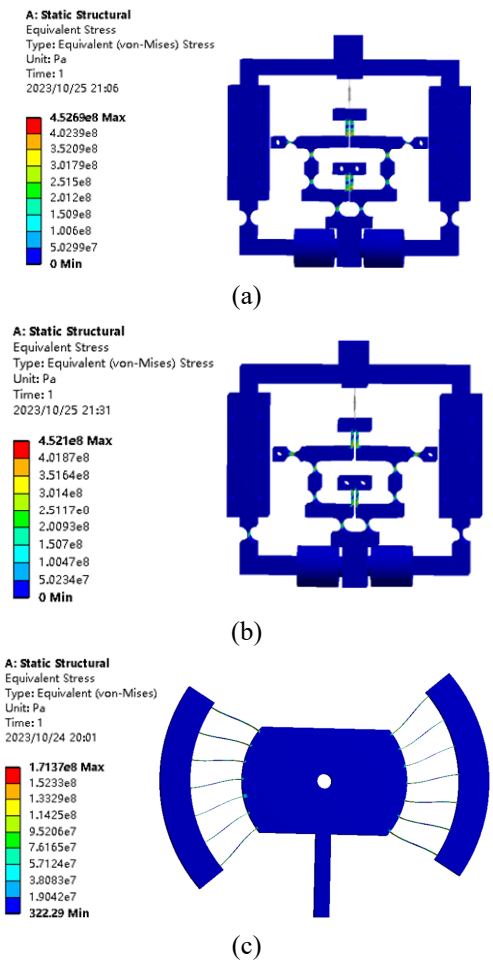

Figure 6: Maximum von Mises stress diagrams. (a) Translational mechanism in non-amplification mode. (b) Translational mechanism in amplification mode. (c) Rotating mechanism.

The first and second modal analysis results of the motion adjustment mechanism are shown in Fig. 7. It can be seen that the first natural frequency is 130 Hz. The overall structure has high stiffness and meets the stability requirements of precision instruments.

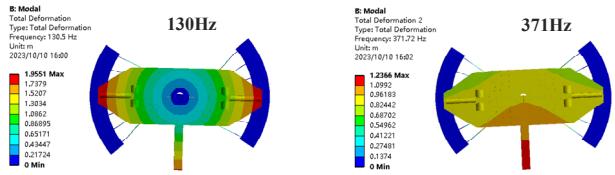

(a) (b)

Figure 7: The first two modal analysis results of motion adjustment mechanism. (a) First order modal shape. (b) Second order modal shape.

To achieve the main goal of maintaining a beam size between 5 - 10 µm in both the horizontal and vertical directions, the position drift of the secondary source slits should be less than 0.5 µm. The secondary source slit structure is made of marble support and invar alloy frame. If the ambient temperature fluctuates ± 0.1°C within 24 h, it will lead to a drifting of up to 0.3 µm in the vertical direction (more severe than the horizontal one). Considering a relative worse condition, the disturbance of the ground vibration on the optical components is 0.4 µm. Thus the total error is 0.5 µm. Therefore, in order to ensure that the position instability of the secondary source slit less than 10 % of the beam size, the ambient temperature stability should be kept at least within ± 0.1°C.

CONCLUSION

A new high-precision secondary source slit is designed, which is characterized with a large opening size of 400 µm and single nano resolution. The first natural frequency of the optimized hinge mechanism has reached 130 Hz, which is of good stiffness. A slit prototype will be done based on the design in the near future.

REFERENCES

[1] Longlife Lee, Chien-Hung Chang, Liang-Jen Huang, *et al.*, "Design and Application of a Mono-beam Slit System at Taiwan Photon Source", *AIP Conference Proceedings*, vol. 2054, no. 1, p. 060054, 2019. doi:10.1063/1.5084685

[2] Hong-Yi Yan, Chien-Hung Chang, Chun-Yu Chen, *et al.*, "Mechanical Design of Secondary Source Slits for Hard X-ray Beam-lines at Taiwan Photon Source", in *Proc. MEDSI'16*, Barcelona, Spain, Sep. 2016, pp. 12-14. doi:10.18429/JACoW-MEDSI2016-MOPE05